J Mol Model (2012) 18:825–834
DOI 10.1007/s00894-011-1108-2

ORIGINAL PAPER

Four-component pharmacophore model for endomorphins toward μ opioid receptor subtypes

Yng-Ching Wu · Tim Jaglinski · Jin-Yuan Hsieh · Jia-Jyun Chiu · Tzen-Yuh Chiang · Chi-Chuan Hwang

Received: 14 January 2011 / Accepted: 25 April 2011 / Published online: 27 May 2011

Abstract In the present work, a series of simulation tools were used to determine structure-activity relationships for the endomorphins (EMs) and derive μ-pharmacophore models for these peptides. Potential lowest energy conformations were determined in vacuo by systematically varying the torsional angles of the Tyr^1-Pro^2 (ω_1) and Pro^2-Trp^3/Phe^3 (ω_2) as tuning parameters in AM1 calculations. These initial models were then exposed to aqueous conditions via molecular dynamics simulations. In aqueous solution, the simulations suggest that endomorphin conformers strongly favor the *trans*/*trans* pair of the ω_1/ω_2 amide bonds. From two-dimensional probability distributions of the ring-to-ring distances with respect to the pharmacophoric angles for EMs, a selectivity range of μ_1 is ca. 8.3~10.5 Å for endomorphin-2 and selectivity range of μ_2 is ca. 10.5~13.0 Å for endomorphin-1 were determined. Four-component μ-pharmacophore models are proposed for EMs and are compared to the previously published δ- and κ-pharmacophore models.

Keywords AM1 calculations · Endomorphin · Molecular dynamics · Pharmacophore

Y.-C. Wu · T. Jaglinski · C.-C. Hwang (✉)
Biomedical Engineering Program, Department of Engineering Science, National Cheng Kung University,
Tainan 70101, Taiwan
e-mail: chchwang@mail.ncku.edu.tw

J.-Y. Hsieh
Computer Science Program, Department of Mechanical Engineering, Ming Hsin University of Science and Technology,
Hsinchu 30401, Taiwan

J.-J. Chiu
Biomolecular Network Program, Department of Electrical Engineering, National Cheng Kung University,
Tainan 70101, Taiwan

T.-Y. Chiang
Neuroscience Program, Department of Life Science,
National Cheng Kung University,
Tainan 70101, Taiwan

Introduction

It is well established that the δ, μ, and κ receptors are the primary locations where opiate drugs exert their influence [1–3]. It has been shown that the μ-selective agonists display the most potent antinociceptive activity, and further, of the known mammalian opioids, the endogenous peptides endomorphin-1 (EM1; Tyr-Pro-Trp-Phe-NH2) and endomorphin-2 (EM2; Tyr-Pro-Phe-Phe-NH2) exhibit the highest selectivity and binding affinity toward the μ-opioid receptor (MOR) [4, 5]. Hence, EM1 and EM2, as well as their derivatives, have been studied extensively to determine their structure-activity relationships (SAR) with the intent to design efficient analgesics with minimal side effects [6, 7].

Even though EM1 and EM2 have been targeted as model peptides, details of their three-dimensional structures and binding sites are still unclear. This is attributed to the fact that baseline solution and membrane-bound structural conformations of EM1 and EM2 were determined through various theoretical and experimental methods in different environments [8–13]. Not only do discrepancies exist among the currently accepted bioactive endomorphin conformation models, these models may not reflect the true in vivo conformation.

In opioid peptides, it is generally accepted that the most important pharmacophoric parameters are the distances from the protonated amine to the Tyr^1 aromatic ring, the distance from the protonated amine to the hydrophobic center and the distance from the Tyr^1 ring to the

hydrophobic center [14]. However, EM1 and EM2 possess two hydrophobic centers, the Trp^3/Phe^3 and Phe^4 aromatic rings situated at residue positions 3 and 4, and it has been pointed out that the N-terminal protonated amine, the Tyr residue in position 1 and both of the aromatic residues (Trp or Phe) in positions 3 and 4 can be considered pharmacophoric elements [15]. Hence, the usual understanding of the correlation of three-component 3D pharmacophore with bioactivity may not adequately predict the SAR of endomorphins (EMs).

Therefore, the present study attempts to investigate the SAR of EMs in vacuo and in aqueous solution using AM1 calculations and molecular dynamics (MD) simulations, respectively. The structural profiles of EM1 and EM2 in vacuo were examined by conducting a systematic conformer analysis using Spartan program. As a result, we obtained the 13×13= 169 conformers of minimized energy for EM1 and EM2, respectively. Furthermore, in aqueous solution, the lowest energy conformers of EMs obtained from AM1 calculations were further analyzed using MD simulations. The results of these MD simulations suggest a MOR pharmacophore model which uses four-component (**N**, **A**, **B**, **C**) pharmacophoric elements rather than the usual three component system.

Methods

Method overview

Figure 1a and b illustrates the geometric structure, including the rotamers of the backbone and sidechains, for EM1 and EM2, respectively. The computational method used in the present work can be generally outlined as follows. Initial geometric endomorphin models were built using the commercial Spartan analysis package. Molecular mechanics (MM) calculations were used to obtain 169 lowest energy conformations in vacuo by varying the torsional angles of the Tyr^1-Pro^2 (ω_1) and Pro^2-Trp^3/Phe^3 (ω_2) as tuning parameters. Using semi-empirical AM1 calculations, the 169 obtained conformations were further refined. Finally, MD simulations of the refined conformations in aqueous solution were conducted. From the aqueous conformations, the pharmacophore models were derived. For the present calculations, the ω_1 torsional angle was selected as the primary criterion to calculate the conformer profiles since the *cis*/*trans* isomerization occurs at the Tyr^1-Pro^2 amide bonds. The ω_2 torsional angle was selected as reference gauge for calculating two-dimensional energy map.

In vacuo calculations

The initial endomorphin structures were constructed using the Spartan package from Wavefunction. The structural profiles of EM1 and EM2 in vacuo (ε=1) were then examined by conducting a systematic conformer analysis using Spartan program. At the first step, the torsional angles of ω_1 and ω_2 were both specified as 0°, and other rotamers were not restricted during the calculation process. The results of equilibrium conformer show that 1600 conformers for EM1 and 1444 conformers for EM2 were produced through MM calculations using the Merck molecular force field (MMFF), respectively [16, 17]. Only one of these conformers for EM1 and EM2, respectively, having the lowest energy was selected and then the equilibrium geometry by semi-empirical AM1 calculations was further calculated [18]. Subsequently, the torsional angles of ω_1 and ω_2 were mutually rotated by increments of 30°, and repeat the first step. Finally, we can obtain the 13×13=169 conformers of minimized energy for EM1 and EM2, respectively.

In aqueous solution calculations

MD simulations were performed using the GROMACS simulation program using the GROMOS96 (ffG43a1) force field [19, 20]. These simulations assume random atomic velocities consistent with a Maxwellian distribution. The atomic positions and velocities were integrated using the standard Verlet algorithm with a time step of 2 fs and SHAKE [21] to constrain all bond lengths. Simulations were performed at a constant temperature of T=300 K and a constant pressure of P=1 atm (the *NPT* ensemble) using the Berendsen coupling scheme [22] with a dimensionless time constant of 0.2. The particle mesh Ewald method (PME) [23, 24] was adopted to calculate the electrostatic forces, and the non-bonded potentials were truncated using a cutoff radius of 14 Å. The formation of a hydrogen bond between an atomic pair was set to occur if both the bond length (r_{HB}) ≤ 3.5 Å and the bond angle (θ_{HB}) ≤ 30° were satisfied. Coordinates and topologies from the lowest energy conformers of EMs obtained from AM1 calculations were converted using the PRODRG small-molecule topology generator program [25], and further analyzed in the GROMACS package. The EMs were solvated in boxes of SPC water [26] with a minimum distance of 10 Å from any peptide atom to the edge of the box. This resulted in approximately 1420 water molecules in a box of length 35.7 Å for EM1 and 1405 water molecules in a box of length 35.3 Å for EM2. Periodic boundary conditions were implemented.

Results

EM conformations in vacuo

Table 1 summarizes the obtained structural features for the EM1 and EM2 lowest energy conformations determined

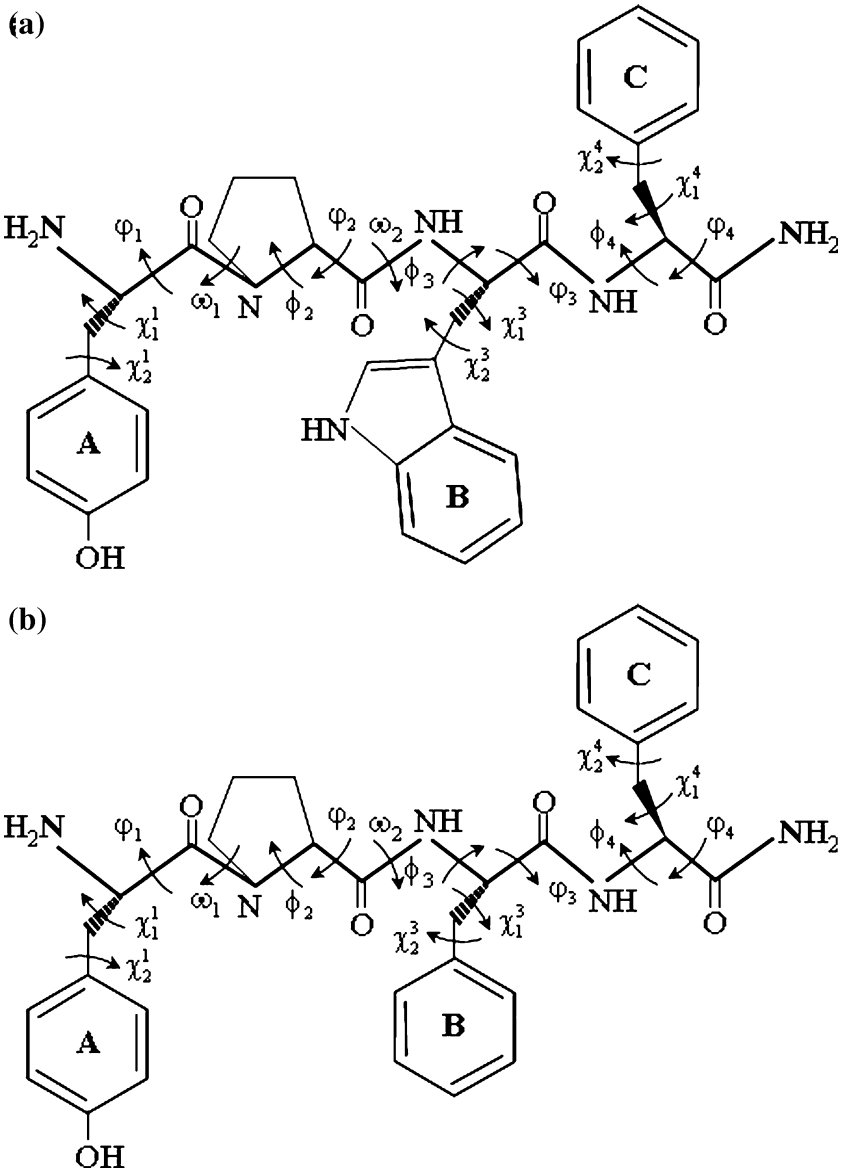

Fig. 1 Schematic of the structural models of EMs. (**a**) EM1. (**b**) EM2. The pharmacophoric elements (red) include protonated nitrogen (**N**), centroid of phenolic group (**A**), and two centroid of hydrophobic groups (**B** and **C**). The key amide bonds are ω_1 and ω_2. The rotamers of the structural backbone and the sidechain are marked

from the present quantum chemistry calculations in vacuo. Included are the amide bond rotamers (ω_1/ω_2), the end-to-end distance (r_{ee}), the probable pharmacophoric distances (**NA**, **NB**, **NC**, **AB**, **AC**, **BC**) and the side chain rotamer angles ($\chi_1^1, \chi_1^3, \chi_1^4$). Our results show that the lower minimized energy conformers of EMs are almost restricted to the conformers of *cis* (~ ±0°) and *trans* (~ ±180°) isomerization regarding the ω_1 and ω_2 rotamers. Nevertheless, EMs bear the lowest energy conformers while both ω_1 and ω_2 rotamers lied on *trans* form. This can be seen from the smoothed, two-dimensional energy maps for EM1 and EM2 (shown as Fig. 2a, b, respectively) constructed from the 169 lowest energy conformations. The lowest energy conformers for

Table 1 Comparison of the lowest-energy conformers of EM1 and EM2 in vacuo using AM1 calculations

	Amide bond rotamer (°)		End-to-end distance (Å)	N-to-ring distance (Å)			Ring-to-ring distance (Å)			Sidechain rotamer (°)		
ligand	ω_1/ω_2		r_{ee}	NA	NB	NC	AB	AC	BC	χ_1^1	χ_1^3	χ_1^4
EM1	trans/trans	180/180	9.85	3.99	8.54	5.96	11.32	6.76	9.58	-56.52	-58.12	-56.77
EM2	trans/trans	180/180	7.76	5.10	10.40	11.63	7.34	8.90	5.44	-172.88	-157.88	-65.35

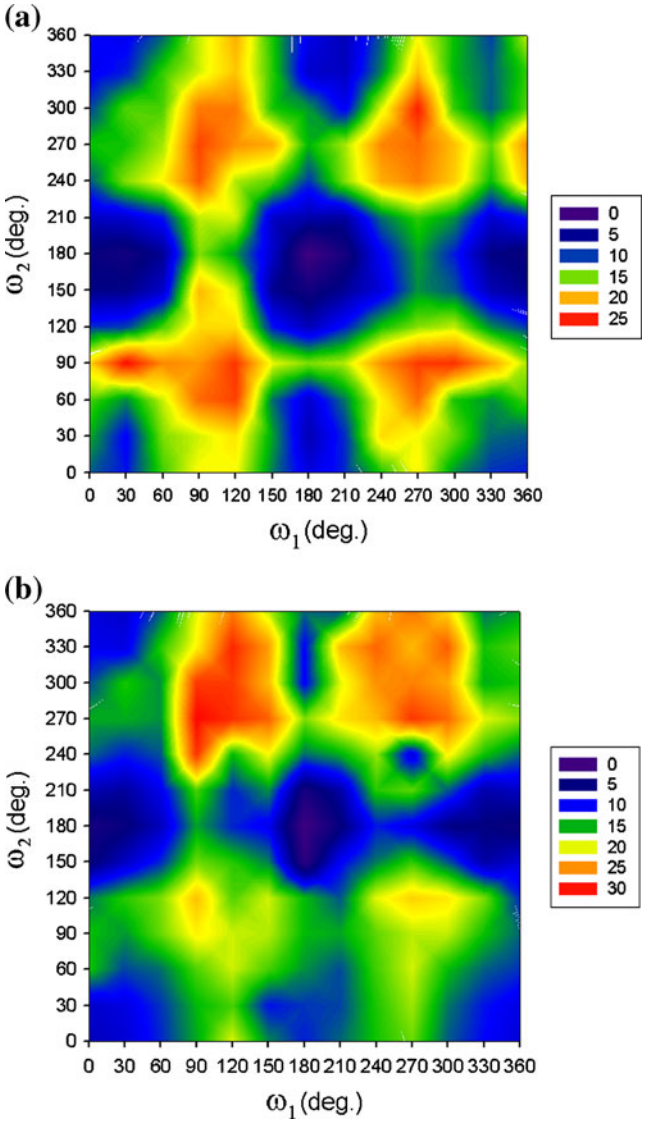

Fig. 2 Conformer energy maps of EMs in terms of the ω_1 and ω_2 torsional angles in vacuo from AM1 calculations. Torsional angles of ω_1 and ω_2 correspond to Tyr^1-Pro^2 and Pro^2-Trp^3/Phe^3 amide bonds, respectively. (**a**) EM1. (**b**) EM2

EM1 and EM2 in vacuo are depicted in Fig. 3. Three intramolecular hydrogen bonds (HBs) are predicted (dashed lines in Fig. 3) and summarized in Table 2. Both EMs possess Trp^3:NH to Tyr^1:CO (3→1) and Phe^4:NH to Pro^2:CO (4→2) intramolecular HBs. EM1 contains a third intramolecular hydrogen bond from the C-terminal NH2 group to the CO group of Trp^3. EM2 also contains a third hydrogen bond from the OH group of the phenolic ring to the backbone CO group of the Phe^3 residue. It was calculated that the $\chi_1^1, \chi_1^3, \chi_1^4$ sidechain angles favor the *gauche* (−) (~ − 60°) and *trans* rotamers in the lowest energy conformers. For EM1, the $(\chi_1^1, \chi_1^3, \chi_1^4)$ rotamers are (*gauche* (−), *gauche* (−), *gauche* (−)), and for EM2 the rotamers are (*trans*, *trans*, *gauche* (−)). Furthermore, as

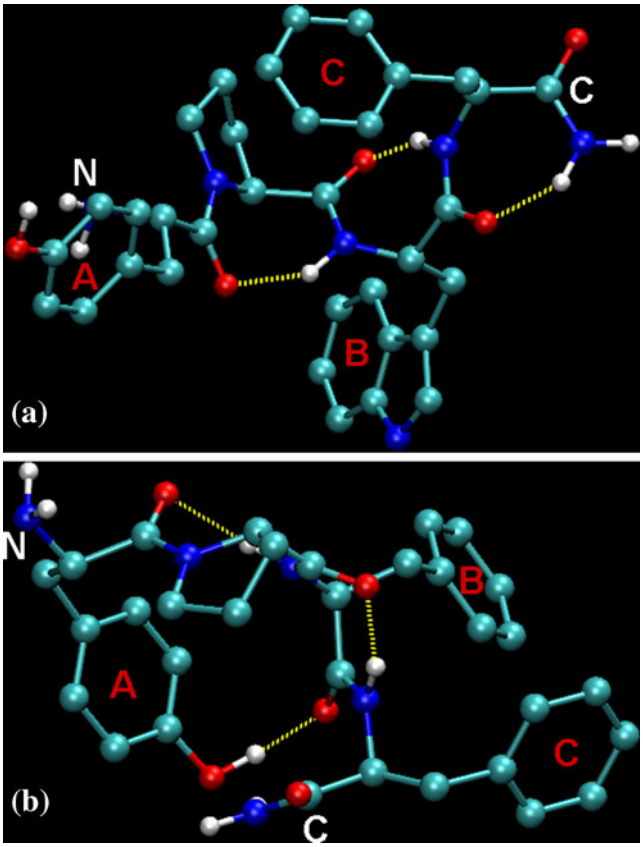

Fig. 3 The lowest energy conformers of EMs in vacuo. (**a**) EM1. (**b**) EM2. Both are at the lowest energy state with three intramolecular HBs shown in yellow dot line

shown in Table 3, it is can be seen that the backbone dihedral angles of EMs reveal the conformers characterized by a 3→1 inverse γ-turn and a 4→2 regular γ-turn with respect to AM1 calculations.

EM conformations in aqueous solution

In regards to structural stability, time histories of the root-mean-square-deviation (RMSD) value of the EMs backbone atoms (Fig. 4a) and the end-to-end distances (r_{ee}) (Fig. 4b) show that stable structures are obtained for both EMs in 2 ns or less of simulation time. After the full

Table 2 Existence of hydrogen bonds in vacuo

Ligand	Donor residue → acceptor residue
EM1	3 → 1
	4 → 2
	C-terminal NH_2 group → CO group of Trp^3 residue
EM2	3 → 1
	4 → 2
	OH group of phenolic ring → CO group of Phe^3 residue

Table 3 Comparison of all the dihedral angles (°) of EMs in vacuo and in aqueous solution using AM1 calculations and MD simulations, respectively

		Backbone chain				Sidechain			
		φ		ψ		χ^1		χ^2	
		AM1	MD	AM1	MD	AM1	MD	AM1	MD
Tyr^1	EM1	–	–	72.89	-17.21	-56.52	-66.70	119.91	97.23
	EM2	–	–	93.37	103.31	-172.88	-174.43	74.23	76.27
Pro^2	EM1	-76.83	-45.43	56.89	113.50	–	–	–	–
	EM2	-79.83	-45.61	51.30	107.61	–	–	–	–
Trp^3	EM1	64.49	-84.90	-47.46	123.53	-58.12	-65.17	-76.78	-90.46
Phe^3	EM2	69.81	58.87	-57.99	-87.83	-157.88	-65.05	87.72	99.16
Phe^4	EM1	75.73	-136.22	-47.81	-44.18	-56.77	-66.27	110.41	106.08
	EM2	-92.71	-62.87	85.62	139.42	-65.35	-72.94	100.20	88.05

simulation time of 10 ns, only the (~ ± 180°) *trans* ω_1 conformation is obtained (Fig. 5c) and r_{ee} converges to average values of ca. 11.0 and 7.4 Å for EM1 and EM2, respectively.

Based upon the geometric criteria for the establishment of a hydrogen bond, EM1 has a 3 → 1 intramolecular hydrogen bond in aqueous solution (Fig. 5a). The average value of 3.5 Å between the Phe^4:NH and Pro^2:CO functional groups, i.e., 4 → 2 intramolecular hydrogen bond, suggests that a second hydrogen bond forms here as well, however, some uncertainty exists in this conclusion

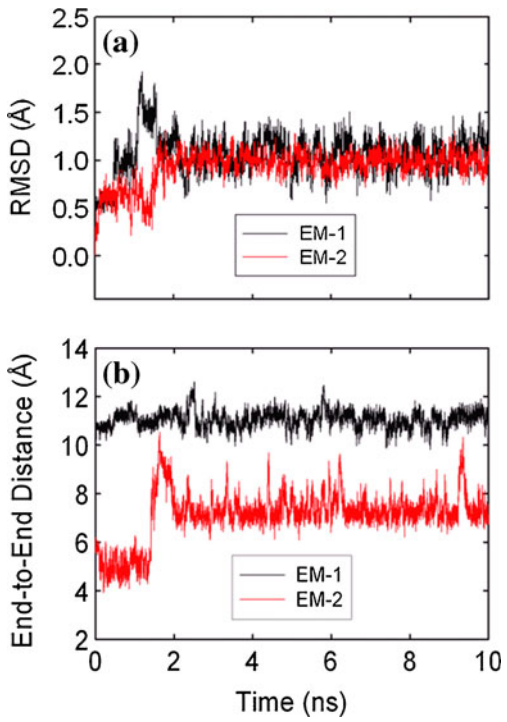

Fig. 4 The structural stability of EMs in aqueous solution. (**a**) The RMSD value of the backbone atoms corresponding to the initial structure obtained from AM1 calculations. (**b**) The variations of end-to-end distances. The distance is defined from the N-terminal nitrogen atom to C-terminal nitrogen atom

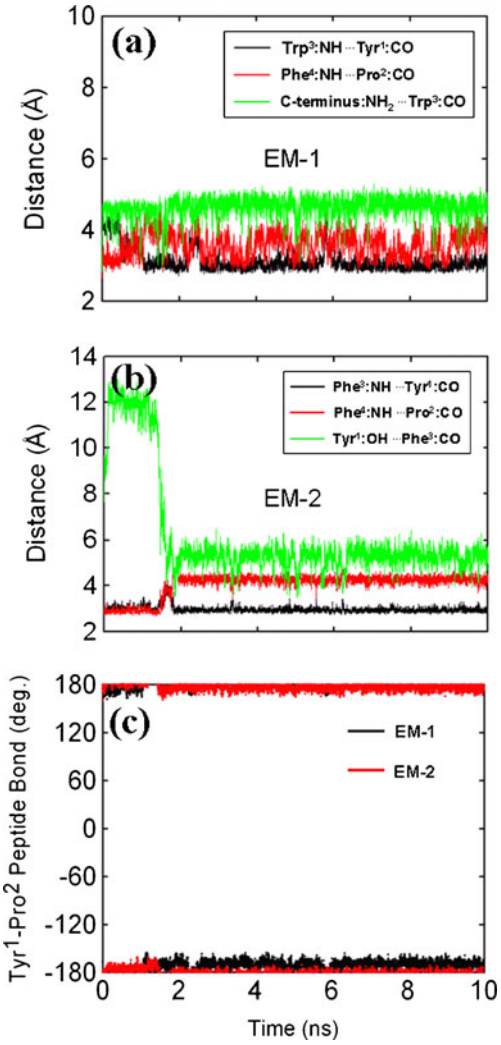

Fig. 5 MD simulations results for dynamic behavior of EMs in aqueous solution. (**a**) The variation of intramolecular HBs over time for EM1. (**b**) The variation of intramolecular HBs over time for EM2. (**c**) The time evolution of torsional angles of Tyr^1-Pro^2 peptide bond (ω_1) for Ems

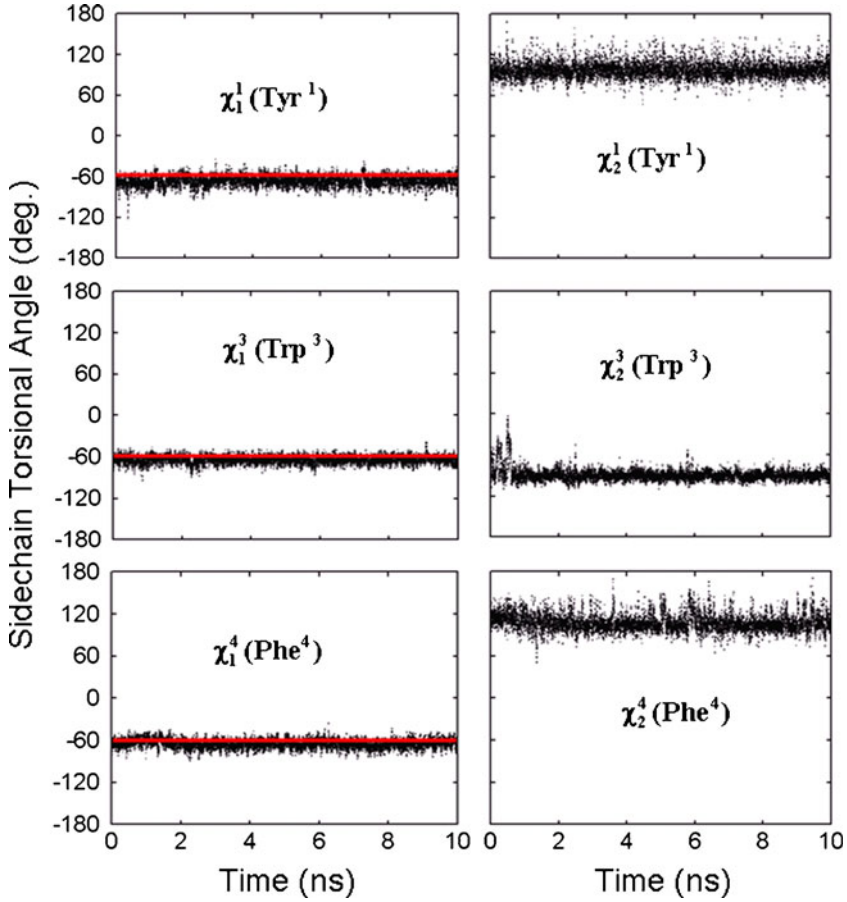

Fig. 6 Time evolutions of sidechain orientations expressed in terms of χ_1 and χ_2 angles for selected residues for EM1. Horizontal lines indicate corresponding values of the lowest energy conformer for EM1 as computed by AM1 calculations. It can be seen that theχ_1^1, χ_1^3 andχ_1^4 angles all favor the *gauche* (−) rotamers in the stable structure

due to the calculation noise. In contrast to EM1, EM2 possesses only the 3 → 1 intramolecular hydrogen bond. The third intramolecular hydrogen bond predicted by AM1 calculations for EMs is absent in aqueous solution (Fig. 5b). Furthermore, no new HBs are formed during the MD simulations.

Table 3 also summarizes the obtained structural features for the EM1 and EM2 stable conformations determined from the present MD simulations in aqueous solution including the backbone and sidechain rotamers. For backbone dihedral angles, it can be seen that EM1 exhibits a 3 → 1 inverse γ-turn, as well as a 4 → 2 inverse γ-turn against regular γ-turn from AM1 calculations. In contrast, only a 3 → 1 inverse γ-turn is present in EM2. On the other hand, it is well-known that the χ_1 rotamers of aromatic rings (e.g., Tyr and Phe) play an essential role in determining the pharmacological activity. Consequently, the sidechain (χ_1^1, χ_1^3, χ_1^4) distributions of EM1 and EM2 in aqueous solution are analyzed as a function of time, as shown in Figs. 6 and 7, respectively. In Figs. 6 and 7, the horizontal lines indicate corresponding values of the lowest energy conformers for EMs as computed by AM1 calculations. In regards to structural stability, the results show that the (χ_1^1, χ_1^3, χ_1^4) rotamers prefer (*gauche* (−), *gauche* (−), *gauche* (−)) for EM1 in aqueous solution that are similar to those observed in vacuo, whereas these rotamers prefer (*trans*, *gauche* (−), *gauche* (−)) for EM2 in aqueous solution that only the χ_1^3 rotamer dramatically varies against AM1 calculations.

Four-component μ-pharmacophore model

Since EMs bear three significant pharmacophoric rings (Tyr[1], Trp[3]/Phe[3], Phe[4]), four-component (**N**, **A**, **B**, **C**) pharmacophore models, based on the stable conformations in aqueous solution, are proposed for EM1 and EM2 (Fig. 8). Many of the possible distances between the endomorphin rings or functional groups fits within the framework of the two-ring models, suggesting that these EMs can bind to many receptors. For two-ring models of receptor selectivity, it has been suggested that aromatic ring separations of 10~13 Å are required for MOR activity [27, 28], 5.7~8.3 Å are required toward the δ opioid receptor (DOR) [29] and 5.0~5.4 Å are required for all three subtypes toward the κ opioid receptor (KOR) [30] immediately eliminating several distances. Further, since it is known from experimental evidence that EMs exhibit the highest selectivity and binding affinity toward the MOR, the calculations which predict that the average value of ring-to-ring distance **AC** (d(**AC**)) is ca. 12 Å for EM1 and

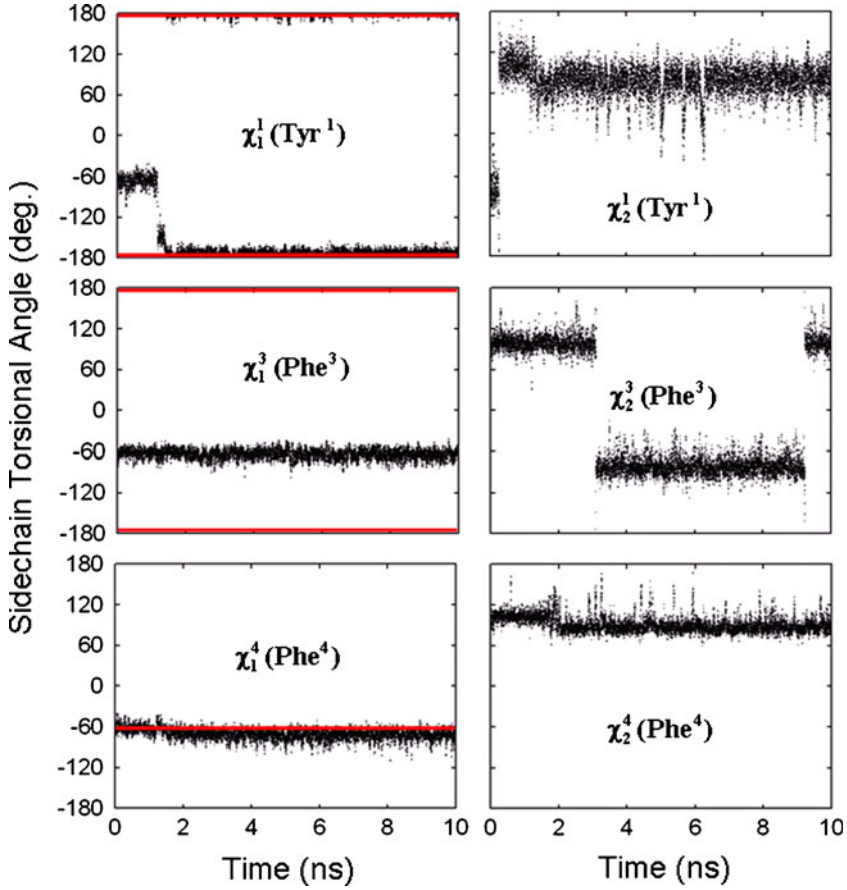

Fig. 7 Time evolutions of sidechain orientations expressed in terms of χ_1 and χ_2 angles for selected residues for EM2. Horizontal lines indicate corresponding values of the lowest energy conformer for EM2 as computed by AM1 calculations. It can be seen that theχ_1^3 andχ_1^4 angles favor the *gauche* (−) rotamers, and χ_1^1 angles favor the *trans* rotamers in the stable structure, significantly different from EM1

that ring-to-ring distance **AB** (d(**AB**)) is ca. 9.4 Å for EM2. However, to fully characterize the peptides, the four-component model proposed here is needed.

Discussion

As previously mentioned, EMs possess the highest selectivity and binding affinity toward the MOR, which has a selectivity range of 10–13 Å regarding two aromatic rings. However, there is biochemical and pharmacological evidence suggesting that MOR can be divided into the μ_1 and μ_2 subtypes [5, 31, 32]. In fact, experimental studies also further indicated that EM1 binds to μ_2 and that EM2 binds to μ_1 [5, 32]. Moreover, previous study has reported that overlap between DAMGO and EM1 conformers show the Tyr^1-MePhe^4 of DAMGO and Tyr^1-Phe^4 of EM1 can assume a similar orientation with a separation between the aromatic rings of ca. 12 Å [27], simultaneously, the results also suggested the Phe^4 residue of EM1 adopts a bioactive conformation at the receptor site and the Trp^3 residue appears as an additional site. On the other hand, in order to clarify the role of Phe^3 and Phe^4 of EM2 in receptor binding, prior research has designed and synthesized a series of analogs in which these Phe residues were replaced by various amino acids [33]. The result indicated that Phe^3 residue has much stronger activity than Phe^4 residue. As mentioned above in connection with different binding characteristics toward the MOR subtypes for EMs, suggest that **N**, **A**, and **C** are the pertinent pharmacophoric elements of EM1, whereas **N**, **A**, and **B** are the pharmacophoric elements of EM2 (see the thick lines of Fig. 8).

The actual selectivity ranges between the aromatic rings for the MOR subtypes have not yet been determined, however, the size distributions of the d(**AC**) and d(**AB**) determined in our calculations could reveal possible binding selectivities for the different μ_1 and μ_2 subtypes. Lissajous construction of the 10 ns simulation time-histories results in the two-dimensional (2D) probability distributions of the distances **AB**/**C** (d(**AB**) for EM2 and d(**AC**) for EM1) against the endomorphin pharmacophoric angles shown in Fig. 9. In Fig. 9c, the designation for angle NB/CA stands for ∠NBA for EM2 and ∠NCA for EM1; similarly for the other angles. From the 2D distributions, the majority of the distribution range for d(**AC**) in EM1 is ca. 10.5~13.0 Å (blue), similarly, the range for d(**AB**) in EM2 is ca. 8.3~10.5 Å (red). Our finding suggests the selectivity ranges for μ_1 and μ_2 are ca. 8.3~10.5 Å and 10.5~13.0 Å, respectively.

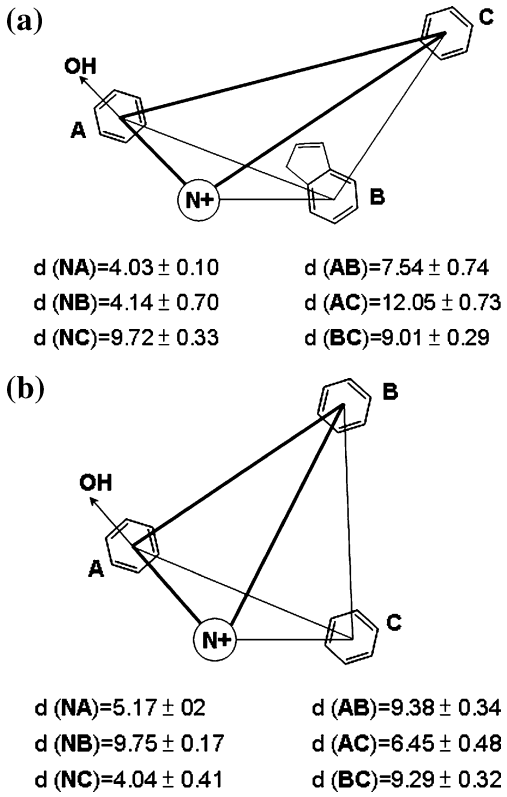

Fig. 8 The four-component μ-pharmacophore models developed for (**a**) EM1. (**b**) EM2. The pairwise distances and the variance values between these four pharmacophore components are shown

In regards to the accuracy of the present simulations in aqueous solution, some connection with reality must be made to show that the bioactive aqueous solution conformations calculated in the present work are reasonable. First, the *trans* only ω_1 bioactive conformation predicted here is consistent with prior researches [10, 13, 34]. In addition, the intramolecular hydrogen bond binding and backbone structure behaviors predicted here are also in agreement with previous studies [10, 11, 34]. On the other hand, the results of sidechain orientations for structurally stable features of EMs indicate that the χ_1^1 rotamer of EM1 favors *gauche* (−), whereas EM2 favors *trans*. During the simulation time period of 10 ns, the initial χ_1^1 rotamer of EM2 adopts *gauche* (−) orientation, and after few ns (ca. 1.5 ns), it rapidly varies to *trans* orientation and remains the value to the end of simulation. This dynamic process also directly affects the interaction between the Tyr[1]:OH and Phe[3]:CO functional groups. As a result, this distance interaction rapidly drops to about 5 Å at around 1.5 ns (see Fig. 5b). However, these results are in agreement with the findings of previous studies which indicated the Tyr[1] prefers to accommodate both the *trans* and *gauche* (−) sidechain orientations [35]. Furthermore, in the present study, the *gauche* (−) orientations for both theχ_1^3 and χ_1^4 rotamers have also been suggested for EMs and their analogues [36–38]. The main tri-rotamer-combinations (χ_1^1, χ_1^3, χ_1^4) of sidechain rotamers of the Tyr[1], Trp[3] and Phe[4] residues for EM1 and the Tyr[1], Phe[3] and Phe[4] residues for EM2 have been identified in χ_1 conformational space [36]. The considerable results indicated that four types of these combinations exist in the conformers of all types of EMs, i.e., (*gauche* (−), *gauche* (−), *gauche* (−)), (*trans*, *gauche* (−), *gauche* (−)), (*gauche* (−), *gauche* (−), *trans*), and (*trans*, *trans*, *gauche* (−)). Indeed, our results show that the tri-rotamer-combinations of EMs are in agreement with previous studies.

Despite these consistencies with previous work, some debate still exists about the detailed structure information and binding sites of these EMs. For example, peptide structures are determined experimentally using cryo-electron microscopy. This technique can only reveal conformation snapshots at temperatures much lower than in the human body and it is not clear how much the

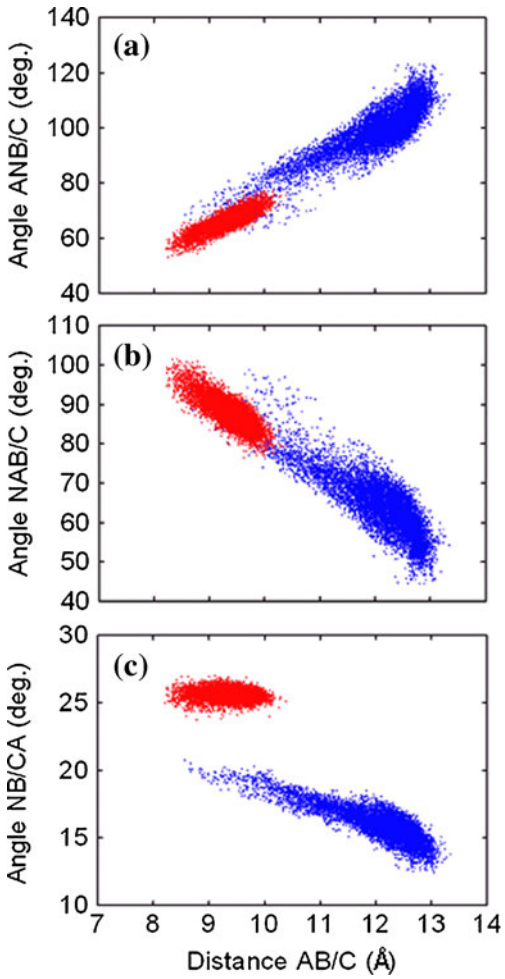

Fig. 9 2D probability distributions of the distances against the pharmacophoric angles for EMs. The distance **AC** for EM1 is shown in blue color, whereas distance **AB** for EM2 is shown in red color. The angle NB/CA stands for ∠NBA for EM2 and ∠NCA for EM1; similar for other angles

cryogenic conformations deviate from those in vivo. Our simulations can demonstrate this, though somewhat indirectly. Quantum chemistry calculations are conducted at 0 K in vacuo. In the present work, three hydrogen bonds, which effect ring distances, were predicted for both EM1 and EM2 in vacuo, however several of these bonds were not predicted in aqueous solution. Though not totally accurate, our quantum chemistry calculations and subsequent MD simulations do provide realistic estimates of in vivo conditions.

It is acknowledged that the models used herein do not completely capture the physical situation in vivo. For example, conformation changes incurred from interactions of the EMs in the locality of the receptors were not modeled. Inclusion of the receptors into the models, though warranted, was not sensible based on the computing power available. As for the flexibility of linear peptides, conformers other than the ones calculated here could exist in vivo. The lowest energy conformers determined from the quantum chemistry calculations only provide initial estimates of the peptide configurations. However, the MD simulations in aqueous do include thermal fluctuations, which are necessary to overcome energy barriers between possible lower energy states. Hence, the MD simulations explore a large energy space. From our analysis, gross changes to the overall structures do not occur through the course of the MD simulations suggesting that the structures determined from quantum chemistry calculations are close to their lowest energy configuration. However, for a sensible pharmacophore model, accurate determination of the distances between rings and other functional groups is required since the ranges for receptor selectivity are not widely separated. This is provided via MD simulations. The four-component model presented in the present work is intended to be a starting point as no model yet exists for these peptides. The distances presented here should be verified through future experimental research.

Conclusions

In this study, we have identified the SAR of EMs in vacuo and in aqueous solution using AM1 calculations and MD simulations, respectively. In vacuo, it was found that the most stable conformers for both the EM1 and EM2 endogenous opioid peptides contain three intramolecular hydrogen bonds. Furthermore, it is can be seen in Table 3, the backbone dihedral angles of EMs reveal the conformers characterized by a 3→1 inverse γ-turn and a 4→2 regular γ-turn, meanwhile, it has been shown that the $\chi_1^1, \chi_1^3, \chi_1^4$ sidechain angles favor the *gauche* (−) and *trans* rotamers in the lowest energy conformers. For EM1, the ($\chi_1^1, \chi_1^3, \chi_1^4$) rotamers are (*gauche* (−), *gauche* (−), *gauche* (−)), and for EM2 the rotamers are (*trans*, *trans*, *gauche* (−)). In aqueous solution, EM1 appears for the 3→1 and 4→2 intramolecular hydrogen bonds based on the conformational stability. By contrast, EM2 possesses only the 3→1 intramolecular hydrogen bond. For backbone conformational characteristics, EM1 exhibits a 3→1 inverse γ-turn, as well as a 4→2 inverse γ-turn against regular γ-turn from AM1 calculations, whereas EM2 only appears on a 3→1 inverse γ-turn. Furthermore, the results show that the ($\chi_1^1, \chi_1^3, \chi_1^4$) rotamers prefer (*gauche* (−), *gauche* (−), *gauche* (−)) for EM1 that are similar to observed those in vacuo, whereas these rotamers prefer (*trans*, *gauche* (−), *gauche* (−)) for EM2 that only the χ_1^3 rotamer dramatically varies against AM1 calculations. Since the EMs contain three significant pharmacophoric rings (Tyr^1, Trp^3/Phe^3, Phe^4) in their sequences, the four-component (**N**, **A**, **B**, **C**) correlation is proposed. The results indicate that the **N**, **A**, and **C** are the main pharmacophoric elements for EM1, whereas **N**, **A**, and **B** are the pharmacophoric elements for EM2. Finally, from the 2D probability distributions of d(**AC**) for EM1 and d(**AB**) for EM2, our finding suggests the selectivity ranges for μ_1 and μ_2 subtypes are ca. 8.3∼10.5 Å and 10.5 ∼13.0 Å, respectively.

Acknowledgments The current research were supported jointly by the National Research Council of Taiwan and the Core Facilities Laboratory of the Kaohsiung-Pingtung Area and the Taiwan National Science Council under the Contract NSC 96-2221-E-006-305-MY2. In addition, we are greatly indebted to Professor Yun-Che Wang for his fruitful discussions.

References

1. Clark JA, Liu L, Price M, Hersh B, Edelson M, Pasternak GW (1989) J Pharmacol Exp Ther 251:461–468
2. Harrison LM, Kastin AJ, Zadina JE (1998) Peptides 19:1603–1630
3. Kieffer BL (1999) Trends Pharmacol Sci 20:19–26
4. Zadina JE, Hackler L, Ge LJ, Kastin AJ (1997) Nature 386:499–502
5. Sakurada S, Zadina JE, Kastin AJ, Katsuyama S, Fujimura T, Murayama K, Yuki M, Ueda H, Sakurada T (1999) Eur J Pharmacol 372:25–30
6. Szatmári I, Biyashev D, Tömböly C, Tóth G, Mácsai M, Szabó G, Borsodi A, Lengyel I (2001) Biochem Biophys Res Commun 284:771–776
7. Okada Y, Fujita Y, Motoyama T, Tsuda Y, Yokoi T, Li T, Sasaki Y, Ambo A, Jinsmaa Y, Bryant SD, Lazarus LH (2003) Bioorg Med Chem 11:1983–1994
8. Fiori S, Renner C, Cramer J, Pegoraro S, Moroder L (1999) J Mol Biol 291:163–175
9. In Y, Minoura K, Ohishi H, Minakata H, Kamigauchi M, Sugiura M, Ishida T (2001) J Pept Res 58:399–412
10. In Y, Minoura K, Tomoo K, Sasaki Y, Lazarus LH, Okada Y, Ishida T (2005) FEBS J 272:5079–5097
11. Leitgeb B, Ötvös F, Tóth G (2003) Biopolymers 68:497–511
12. Podlogar BL, Paterlini MG, Ferguson DM, Leo GC, Demeter DA, Brown FK, Reitz AB (1998) FEBS Lett 439:13–20

13. Shao X, Gao Y, Zhu C, Liu X, Yao J, Cui Y, Wang R (2007) Bioorg Med Chem 15:3539–3547
14. Deschamps JR, Flippen-Anderson JL, George C (2002) Biopolymers 66:287–293
15. Gentilucci L, Tolomelli A (2004) Curr Top Med Chem 4:105–121
16. Halgren TA (1996) J Comput Chem 17:490–519
17. Halgren TA (1996) J Comput Chem 17:616–641
18. Dewar MJS, Zoebisch EG, Healy EF, Stewart JJP (1985) J Am Chem Soc 107:3902–3909
19. Lindahl E, Hess B, van der Spoel D (2001) J Mol Model 7:306–317
20. Scott WRP, Huenenberger P, Tironi I, Mark A, Billeter S, Fennen J, Torda A, Huber T, Krueger P, van Gunsteren W (1999) J Phys Chem A 103:3596–3607
21. Ryckaert JP, Ciccotti G, Berendsen HJC (1977) J Comput Phys 23:327–341
22. Berendsen HJC, Postma JPM, van Gunsteren WF, DiNola A, Haak JR (1984) J Chem Phys 81:3684–3690
23. Darden T, York D, Pedersen L (1993) J Chem Phys 98:10089–10092
24. Essmann U, Perera L, Berkowitz ML, Darden T, Lee H, Pedersen LG (1995) J Chem Phys 103:8577–8593
25. Schuettelkopf AW, van Aalten DMF (2004) Acta Crystallogr D Biol Crystallogr 60:1355–1363
26. Berendsen HJC, Postma JPM, van Gunsteren WF, Hermans J (1981) In: Pullman B (ed) Intermolecular forces. Reidel, Dordrecht, pp 331–342
27. Paterlini MG, Avitabile F, Ostrowski BG, Ferguson DM, Porthogese PS (2000) Biophys J 78:590–599
28. Yamazaki T, Pröbsti A, Schiller PW, Goodman M (1991) Int J Pept Protein Res 37:364–381
29. Shenderovich MD, Liao S, Qian X, Hruby VJ (2000) Biopolymers 53:565–580
30. Wu YC, Lin JS, Hwang CC (2007) J Phys Chem B 111:7377–7383
31. Pasternak GW, Wood PL (1986) Life Sci 38:1888–1898
32. Sakurada S, Hayashi T, Yuhki M, Fujimura T, Murayama K, Yonezawa A, Sakurada C, Takeshita M, Zadina JE, Kastin AJ, Sakurada T (2000) Brain Res 881:1–8
33. Honda T, Shirasu N, Isozaki K, Kawano M, Shigehiro D, Chuman Y, Fujita T, Nose T, Shimohigashi Y (2007) Bioorg Med Chem 15:3883–3888
34. Leitgeb B, Szekeres A, Tóth G (2003) J Pept Res 62:145–157
35. Grieco P, Giusti L, Carotenuto A, Campiglia P, Calderone V, Lama T, Gomez-Monterrey I, Tartaro G, Mazzoni MR, Novellino E (2005) J Med Chem 48:3153–3163
36. Leitgeb B, Szekeres A (2003) J Mol Struct THEOCHEM 666–667:337–344
37. Gentilucci L, Tolomelli A, Squassabia F (2007) Protein Pept Lett 14:51–56
38. Tömböly C, Kövér KE, Péter A, Tourwé D, Biyashev D, Benyhe S, Borsodi A, Al-Khrasani M, Rónai AZ, Tóth G (2004) J Med Chem 47:735–743